Physica D 405 (2020) 132399

Contents lists available at ScienceDirect

Physica D

journal homepage: www.elsevier.com/locate/physd

# Explosive, continuous and frustrated synchronization transition in spiking Hodgkin–Huxley neural networks: The role of topology and synaptic interaction

Mahsa Khoshkhou, Afshin Montakhab *

*Department of Physics, College of Sciences, Shiraz University, Shiraz 71946-84795, Iran*

ARTICLE INFO

*Article history:*
Received 3 May 2019
Received in revised form 27 January 2020
Accepted 6 February 2020
Available online 11 February 2020
Communicated by H. Nakao

*Keywords:*
Synchronization
Hodgkin–Huxley neuron
Phase transition
Electrical and chemical synapses
Complex networks

ABSTRACT

Synchronization is an important collective phenomenon in interacting oscillatory agents. Many functional features of the brain are related to synchronization of neurons. The type of synchronization transition that may occur (explosive vs. continuous) has been the focus of intense attention in recent years, mostly in the context of phase oscillator models for which collective behavior is independent of the mean-value of natural frequency. However, synchronization properties of biologically-motivated neural models depend on the firing frequencies. In this study we report a systematic study of gamma-band synchronization in spiking Hodgkin–Huxley neurons which interact via electrical or chemical synapses. We use various network models in order to define the connectivity matrix. We find that the underlying mechanisms and types of synchronization transitions in gamma-band differs from beta-band. In gamma-band, network regularity suppresses transition while randomness promotes a continuous transition. Heterogeneity in the underlying topology does not lead to any change in the order of transition, however, correlation between number of synapses and frequency of a neuron will lead to explosive synchronization in heterogeneous networks with electrical synapses. Furthermore, small-world networks modeling a fine balance between clustering and randomness (as in the cortex), lead to explosive synchronization with electrical synapses, but a smooth transition in the case of chemical synapses. We also find that hierarchical modular networks, such as the connectome, lead to frustrated transitions. We explain our results based on various properties of the network, paying particular attention to the competition between clustering and long-range synapses.


## 1. Introduction

The phenomenon of phase transition is an important part of modern statistical physics with many applications in physical and biological systems [1–4]. It is generally believed that many naturally occurring systems self-organize to the edge of a phase transition point which can lead to many functional advantages [5–7]. In the case of biological systems, such transitions are generally believed to be of the critical (continuous) nature associated with a critical point [8,9] or an extended critical regime [10,11]. Synchronization transition is an interesting phase transition that might occur in some important systems such as power grids [12], ecological systems [13], and seasonal epidemics spreading [14], with both a continuous as well as a more interesting explosive transition. It is also interesting to note that the critical brain hypothesis [9] had originally assumed that the brain operates at the edge of an *activity* phase transition. However, recent theoretical [15,16] as well as experimental [17] studies show that the criticality may be associated with a *synchronization* transition. This possibility provides a stronger motivation to study various types of synchronization transition that may occur in network models of biological neurons.

Phase synchronization also has a key role in large-scale integration, memory, vision and other cognitive tasks performed by the human brain [18–21]. In a healthy brain, synchrony must occur at a moderate level. Excessive synchronization leads to brain disorders like epilepsy or Parkinson, while schizophrenia and autism are related to deficit of synchronization among neurons [22]. Thus a healthy brain is thought to be functioning at the edge of synchronization transition between order and randomness [23,16,15]. From this perspective, a slight increase in neural interactions might lead to a synchronization transition in local neural circuits. The type of resultant transition (continuous, explosive or frustrated) is therefore important. For example, when the emerging transition is a continuous one, then a small change in the interaction strength changes the amount of synchronization slightly. But if the emerging transition is an explosive one a

* Corresponding author.
*E-mail address:* Montakhab@shirazu.ac.ir (A. Montakhab).

https://doi.org/10.1016/j.physd.2020.132399
0167-2789/

small increase in the interaction strength may result in a sudden emergence of global order in the neural circuit. Explosive synchronization has functional advantages if it occurs during a fast response, but it also has disadvantages if it occurs, for example, during an epileptic seizure.

Brain oscillations are categorized in various frequency bands. For example, beta-band (13–30 Hz) are typically associated with cognitive task performance. Recently, we have provided a systematic study of beta-band synchronization transitions in network models of Izhikevich neurons [24] and showed that contrary to the case of simple phase oscillators, biologically meaningful models of neural dynamics exhibit synchronization transitions which depend on the average firing frequency of neurons [24]. This difference is rooted in the fact that phase oscillator dynamics has a single time-scale (the mean-value of natural frequencies) which can be re-scaled without having any significant influence on the dynamics of the network [25], while biologically plausible neural dynamics typically has more than one time-scale, e.g. refractory period. The frequency-dependent behavior can arise when one of these time-scales depends on a changing parameter, while the other one does not, thus leading to changing ratio of the various time-scales [24]. In fact it was shown that the patterns of transition changed significantly when one increased the average frequency to the gamma-band ( $>$ 30 Hz).

Gamma-band oscillations are also an important class of rhythms appearing during a broad range of the brain activities [26], and have received a great deal of attention. Gamma-band oscillations have been observed in several cortical areas, as well as subcortical structures [27]. In sensory cortex, gamma power increases with sensory drive [28], cognitive tasks including feature binding [29], visual grouping [30], stimulus selection [31,32] and attention [33]. In higher cortex, gamma power is the dominant rhythm during working memory [34] and learning [35]. Also, it is reported that irregular gamma waves have been observed in pathologies such as Alzheimer [36].

Our purpose here is to provide a systematic study of a biologically motivated neuronal network. We therefore propose to study synchronization transition in gamma-band and seek the effect of synaptic interaction (chemical vs. electrical synapses) as well as the topology of the network used on the ensuing transition type. However, Izhikevich neurons have a tendency to burst as opposed to spike when one increases the input in order to increase the frequency. Furthermore, increasing interaction strength in network of Izhikevich neurons also leads to bursting behavior. On the other hand Hodgkin–Huxley (HH) neurons have a large stable spiking range in gamma frequencies [37]. We therefore use network models of HH neurons in gamma band in order to study synchronization patterns which emerge.

Although synchronization of HH (or HH-type) neurons has been extensively studied before, e.g. in [38–46], a systematic study of (the order of) synchronization transition has not been performed to the best of our knowledge. In fact, much of such type of studies usually employ phase oscillator models such as the Kuramoto model [47,48]. Here, our emphasis is to ascertain the type of phase transition (e.g. continuous vs. explosive) that may occur in a collection of HH neurons *and* how that may depend on synaptic interaction and/or underlying structure (network) [49]. Surprisingly, we find that one- and two-dimensional lattice networks of spiking HH neurons exhibit no transition. Instead they exhibit quasiperiodic partial synchronization as a result of strong clustering which does not lead to global order due to lack of long-range interactions. Random network structures like Erdos–Renyi (ER) and scale-free (SF) networks exhibit continuous transition with either electrical or chemical synapses, with no significant difference between SF and ER structures. However, small-world network with high clustering coefficient and long-range interaction exhibits explosive (first-order) transition to synchronization when neurons interact via electrical synapses, but exhibits continuous (second-order) transition when interacting via chemical synapses. Furthermore, we consider the role of heterogeneity by introducing a correlation between frequency and the degree of a given neuron. We find that while heterogeneity (in degree or frequency) does not change the order of continuous transition, a correlation between the two can lead to explosive synchronization with electrical synapses, but not with chemical synapses. Finally, we show that hierarchical modular (HM) networks with both types of synapses exhibit frustrated synchronization in an intermediate regime between disordered and ordered phases of the system. Some of the structures studied here have been studied in the beta-band and will consequently be compared and contrasted. However, the case of correlated heterogeneity as well as HM networks are just included in the current study and their counterparts in beta-band had not been studied in Ref. [24]. Consequently, such results can be compared with those of phase oscillators independent of frequency.

In the following section, we describe the model we use for our study. In Section 3, we describe our simulation details including the numerical methods used. Extensive results of our numerical study are presented in Section 4, and we close the paper with some concluding remarks in Section 5.

## 2. Model

Consider $N$ Hodgkin–Huxley neurons on an arbitrary network. Electrical activity of $i$th neuron of the network is described by a set of four nonlinear coupled ordinary differential equations as follows [37]:

$$C_m \frac{dv_i}{dt} = I_i^{DC} + I_i^{syn} - G_{Na} m_i^3 h_i (v_i - V_{Na}) - G_K n_i^4 (v_i - V_K) - G_L (v_i - V_L) \tag{1}$$

$$\frac{dm_i}{dt} = \alpha_m(v_i)(1 - m_i) - \beta_m(v_i) m_i \tag{2}$$

$$\frac{dh_i}{dt} = \alpha_h(v_i)(1 - h_i) - \beta_h(v_i) h_i \tag{3}$$

$$\frac{dn_i}{dt} = \alpha_n(v_i)(1 - n_i) - \beta_n(v_i) n_i \tag{4}$$

for $i = 1, 2, \ldots, N$. Here $v_i$ is the membrane potential, $m_i$ and $h_i$ are variables for activation and inactivation of sodium current, and $n_i$ is the variable for activation of potassium current [37]. $\alpha$ and $\beta$ functions are the so-called rate variables of HH neuron for each type of ionic currents and depend on the instantaneous membrane potential [37]. We use $C_m = 1.0$, $G_{Na} = 120$, $G_K = 36$, $G_L = 0.3$, $V_{Na} = 50$, $V_K = -77$ and $V_L = -54.387$ for the constant parameters [38]. $I_i^{DC}$ is an external current which differs from a neuron to the other and determines dynamical properties of uncoupled HH neurons. It is shown that for $I^{DC} > 9.8$ $\mu$A/cm$^2$ a stable limit-cycle is the global attractor for a single HH neuron [50]. We choose values of $I_i^{DC}$ randomly from a Poisson distribution with mean value 10.0 $\mu$A/cm$^2$. Therefore, intrinsic firing rates are non-identical and most of the neurons spike regularly with gamma rhythms [26]. Here, we set the mean intrinsic firing rate is $f \simeq 75$ Hz, unless otherwise stated.

The term $I_i^{syn}$ in Eq. (1) represents synaptic current received by post-synaptic neuron $i$. Functional form of this current depends on the synaptic type. For a gap junction or an electrical synapse the synaptic current is [51]:

$$I_i^{syn} = \frac{1}{D_i} \sum_j g_{ji} (v_j - v_i) \tag{5}$$

and if the synapse is chemical then [51]:

$$I_i^{syn} = \frac{1}{D_i}\sum_j g_{ji}\frac{exp(-\frac{t-t_j}{\tau_s}) - exp(-\frac{t-t_j}{\tau_f})}{\tau_s - \tau_f}(V_0 - v_i) \quad (6)$$

where $D_i$ is in-degree of node $i$, $g_{ji}$ is the strength of synapse from pre-synaptic neuron $j$ to post-synaptic neuron $i$. Here we assumed that all existing synapses have the same strength, viz $g_{ji} = ga_{ji}$, where $g$ is the electrical conductance of synapse and $a_{ji}$ is the element of adjacency matrix of the underlying network. Also in Eq. (6) $t_j$ is the instance of last spike of pre-synaptic neuron $j$, $\tau_s$ and $\tau_f$ are the slow and fast synaptic decay constants and $V_0$ is the reversal potential of synapse which is equal to zero since we assumed that all synapses in our circuit are excitatory. In this study we take $\tau_s = 1.7$ and $\tau_f = 0.2$ which are the values obtained according to experimental data [51]. From the functional form of these synaptic currents, one can expect that they might have different effects on synchronization of neuronal networks. For example, electrical synapses depend on the phase difference of connected neurons with increasing strength for unsynchronized neurons, while chemical synapses tend to effect post-synaptic neurons regardless of the phase difference, and decaying in strength as a function of time after pre-synaptic firing time $t_j$. Therefore, for example, one would expect for a given value of coupling strength $g$, electrical synapses would provide more synchronization when compared to chemical synapses.

In order to quantify the amount of phase synchronization in a neural population, we assign an instantaneous phase to each neuron as in [52]:

$$\phi_i(t) = 2\pi\frac{t - t_i^m}{t_i^{m+1} - t_i^m} \quad (7)$$

where $t_i^m$ is the instant of $m$th spike of neuron $i$. Then we define a global instantaneous order parameter as:

$$S(t) = \frac{2}{N(N-1)}\sum_{i\neq j} cos^2\Big(\frac{\phi_i(t) - \phi_j(t)}{2}\Big) \quad (8)$$

The global order parameter $S$ is the long-time-average of $S(t)$ at the stationary state and measures collective phase synchronization in oscillations of membrane potentials of all neurons, viz $S = \langle S(t)\rangle_t$. $S$ is bounded between 0.5 and 1. If neurons spike out-of-phase, then $S\simeq 0.5$ where they spike completely in-phase $S\simeq 1$. For states with partial synchrony $0.5 < S < 1$.

Along with the order parameter $S$, we have also calculated the more commonly used Kuramoto order parameter [47]:

$$R(t)e^{i\theta} = \frac{1}{N}\sum_j e^{i\phi_j(t)} \quad (9)$$

with $R = \langle R(t)\rangle_t$ where $0 \leq R \leq 1$. $R = 0$ indicates asynchronous, while $R = 1$ completely synchronous, oscillations. Essentially, the same results are obtained for $R$ as those obtained for $S$. However, from a statistical point of view $R(t)$ represents an average of $N$ data points while $S(t)$ represents an average of $N(N-1)/2$ data points which results in better statistics for our limited system sizes, and therefore better statistics considering our system size limitations. We also define a generalized susceptibility as the relative root-mean-square fluctuations in the given order parameter:

$$\kappa_S = \Big(\frac{\langle S^2(t)\rangle - \langle S(t)\rangle^2}{\langle S(t)\rangle^2}\Big)^{1/2} \quad (10)$$

or:

$$\kappa_R = \Big(\frac{\langle R^2(t)\rangle - \langle R(t)\rangle^2}{\langle R(t)\rangle^2}\Big)^{1/2} \quad (11)$$

Such generalized susceptibilities are very useful tools in order to study phase transitions in general, since critical systems are supposed to exhibit maximal fluctuations at the critical point, diverging in the thermodynamic $N \to \infty$ limit.

## 3. Methods

We have scrutinized transition to phase synchronization in networks with $N$ HH neurons interacting via two different synaptic types. We start by providing a detailed description of our procedure. We first determine the network topology by specifying elements of its adjacency matrix. These elements are either zero or one depending on if the nodes are unconnected or connected, respectively. The links in our networks are symmetric. Synapses are also not plastic in this study. The strength of synapses is set with parameter $g$ explained in the previous section. After constructing each network, the synaptic type is determined. If synapses are supposed to be electrical, we use Eq. (5) to describe synaptic currents. While neurons are assumed to interact via chemical synapses, Eq. (6) is used. Next, we fix the values of $I_i^{DC}$ and set the parameter $g$ equal to zero. We then integrate Eqs. (1)–(4) using fourth order Runge–Kutta method with a fixed time step $\Delta t = 10^{-3}$ ms. Typically, much larger time steps are used in simulations of HH neurons, see for example [40,41]. However, since long relaxation times were required in our studies (particularly near the transition points) we choose such a short time step in order to avoid the accumulation of errors. Using this small time step, we are able to specify $t_i^m$, the instant of $m$th spiking of each neuron with an accuracy of $10^{-3}$ ms. Finally we obtain the phase of all neurons and calculate $S(t)$ and $R(t)$ at every time instant (Eqs. (8) and (9)). We allow the dynamics to progress for a long transient time (order of $10^6$ time steps) until the fluctuations in $S(t)$ or $R(t)$ reach a stationary state. After reaching stationary state, we run our simulation for another $2\times 10^4$ ms ($2\times 10^7$ time steps) and evaluate the order parameter $S$ and $R$ by averaging $S(t)$ and $R(t)$ over this second interval. We next increase the value of $g$ slightly (keeping all other conditions fixed) and repeat the whole process to evaluate $S$ and $R$ again. In this manner we obtain dependence of order parameter on coupling strength $g$, in each network topology and for each of the above mentioned synaptic types. The initial condition of integration are random for $g = 0$ and the system is evolved quasi-statically for larger $g$ values. The synchronization diagrams that are reported here are results of averaging over five network realizations as well as other stochastic parameters. Our results are reported for typically $N \approx 500$, but the limited system size does not seem to be an issue in the results to be presented, as essentially the exact same results was obtained when we changed the system size within the range of our computational limits.

## 4. Results

### 4.1. Regular networks

The first structure that we consider is regular network, a one dimensional ring of size $N = 500$ and the mean connectivity $z = 50$ as well as a two-dimensional lattice of side $L$ ($N = L \times L$) with $L = 22$ and the mean connectivity $z = 16$. The results are shown in Figs. 1(a–d). It is observed that increasing $g$ does not lead to a transition in either case. It is somewhat surprising as one would expect a transition to synchrony for large $g$. We have therefore investigated the raster plots for this system for different $g$ values. Such raster plots for one-dimensional ring with electrical synapses for four values of $g$ are shown in Figs. 1(e–h). Raster plots for rings with chemical synapses are qualitatively the same as Figs. 1(e–h). It is realized that imposing

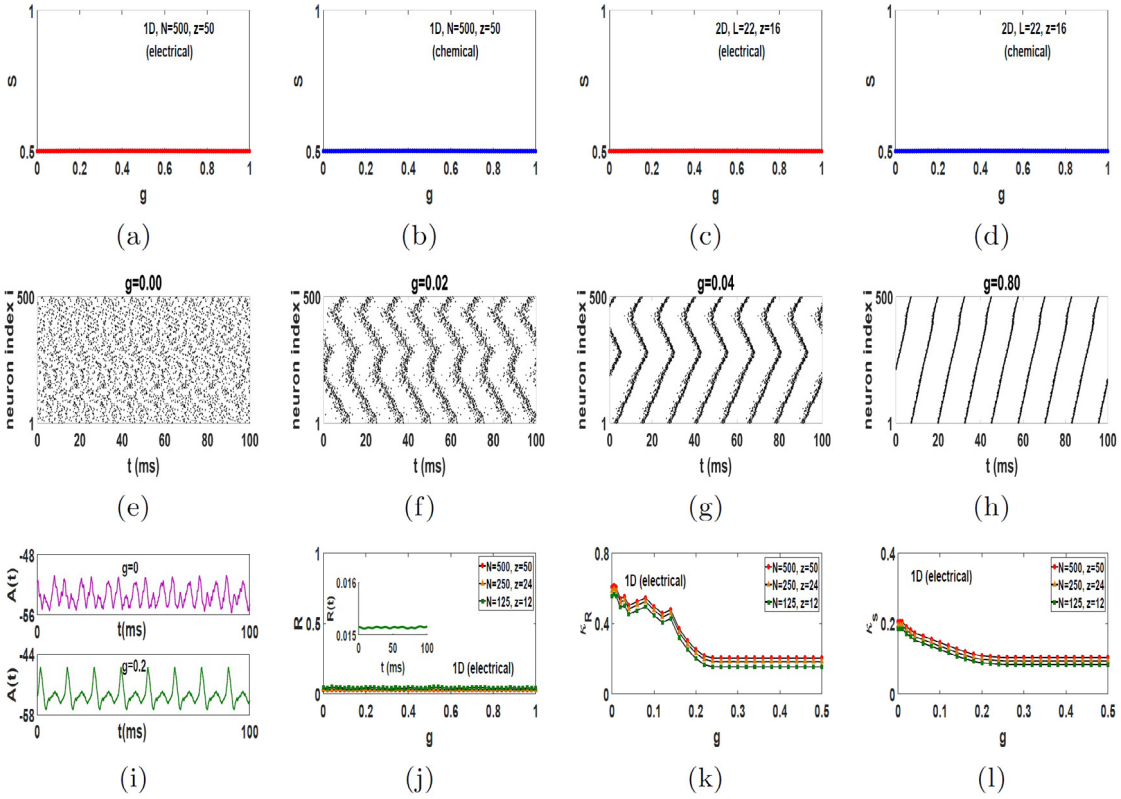


**Fig. 1.** Synchronization diagram of HH neurons on regular networks: (a) and (b) One-dimensional ring with electrical and chemical synapses. (c) and (d) Two-dimensional lattice with electrical and chemical synapses. (e)–(h) Raster plots of the one-dimensional ring with electrical synapses for four values of $g$. (i) Network activity for the system in fully asynchronized (orange curve) and in quasiperiodic partially synchronized (green curve) states. (j) The Kuramoto order parameter $R$ vs $g$ for 1D rings with electrical synapses for different system sizes $N$. The inset shows timeseries $R(t) - t$ for the largest system size and for $g = 0.80$. (k) and (l) The generalized susceptibilities $\kappa_R$ and $\kappa_S$ vs $g$ for the same systems as in (j). $z = 0.1N$ in each case. $t = 0$ indicates the beginning of stationary state. The synchronization diagrams and susceptibility plots show the averaged results over five initial conditions. (For interpretation of the references to color in this figure legend, the reader is referred to the web version of this article.)

a small interaction among neurons in a regular ring leads to formation of correlated regions. This is not unexpected since regular rings have high clustering coefficient [25]. Increasing $g$ slightly, regulates the phase of neurons on a local level. Since there are no long-range synapses in the system, further increase of $g$ could not vanish phase lags among neurons belonging to far away areas of the network, but instead results in the emergence of the so-called quasiperiodic partial synchronization. Quasiperiodic partial synchronization is denoted to the state of a population of interacting oscillators in which the system sets into a nontrivial dynamical regime where oscillators display quasiperiodic dynamics while collective observable of the system oscillate periodically [53–55]. A relevant collective observable for a neural network is the network activity that is defined as $A(t) = \frac{1}{N}\sum_{i=1}^{N} v_i(t)$. In Fig. 1(i) we have plotted A(t) for a regular ring of HH neurons for $g = 0.00$ when neurons are fully asynchronous (orange curve) and also for $g = 0.80$ which is where the network is in a quasiperiodic partial synchronization state (green curve). It is seen that when neurons spike out of order, $A(t)$ fluctuates irregularly. But when the network is in state of quasiperiodic partial synchronization neurons spike quasiperiodically and $A(t)$ oscillates periodically. This state emerges in the rings from $g \simeq 0.20$ and remains robust when $g$ is increased further as the perspective of raster plots remain qualitatively the same from $g = 0.20$ to $g = 1.00$ (or even for larger values of $g$ which are not shown here).

For sake of comparison, in Fig. 1(j) we show the $R - g$ plot for 1D ring with electrical synapses for three different system sizes $N$. The mean connectivity in each system is set to be $z = 0.1N$. In light of these plots we find that the synchronization diagram remains unaltered upon increasing the system size. Timeseries $R(t) - t$ for the largest system size and for $g = 0.80$ is also illustrated in the inset of Fig. 1(j). Comparing Figs. 1(a) and 1(j) one verifies the equivalence of the results obtained based on the order parameters $R$ and $S$, except for the more refined statistics resulting from $S$. Moreover, the generalized susceptibilities $\kappa_R$ and $\kappa_S$ for the same systems as in Fig. 1(j), are illustrated in Figs. 1(k) and 1(l), respectively. It is observed that increasing $g$ does not lead to any distinctive peak in $\kappa_R$ or $\kappa_s$, confirming that no phase transition occurs in this systems. Generalized susceptibilities for other regular networks studied here are qualitatively similar to Figs. 1(j) and 1(l) (not shown).

We note that one might suspect that the lack of transition observed in the 1D lattice might be due to the low dimensional structure, similar to the lack of phase transition in, for example, 1D Ising model. That is why we have also performed simulations for the 2D $L \times L$ lattice whose main results are shown in Figs. 1(c) and 1(d) which again show no transition. We note that raster plots of the 2D system are quantitatively the same as the 1D case with lesser coherence (due to smaller clustering) and that network oscillations, $A(t)$, are also very similar to the 1D case (not shown).

### 4.2. ER and SF networks

We next consider random networks with small-world effect but with much smaller clustering compared to regular networks. We consider ER network which has a homogeneous random

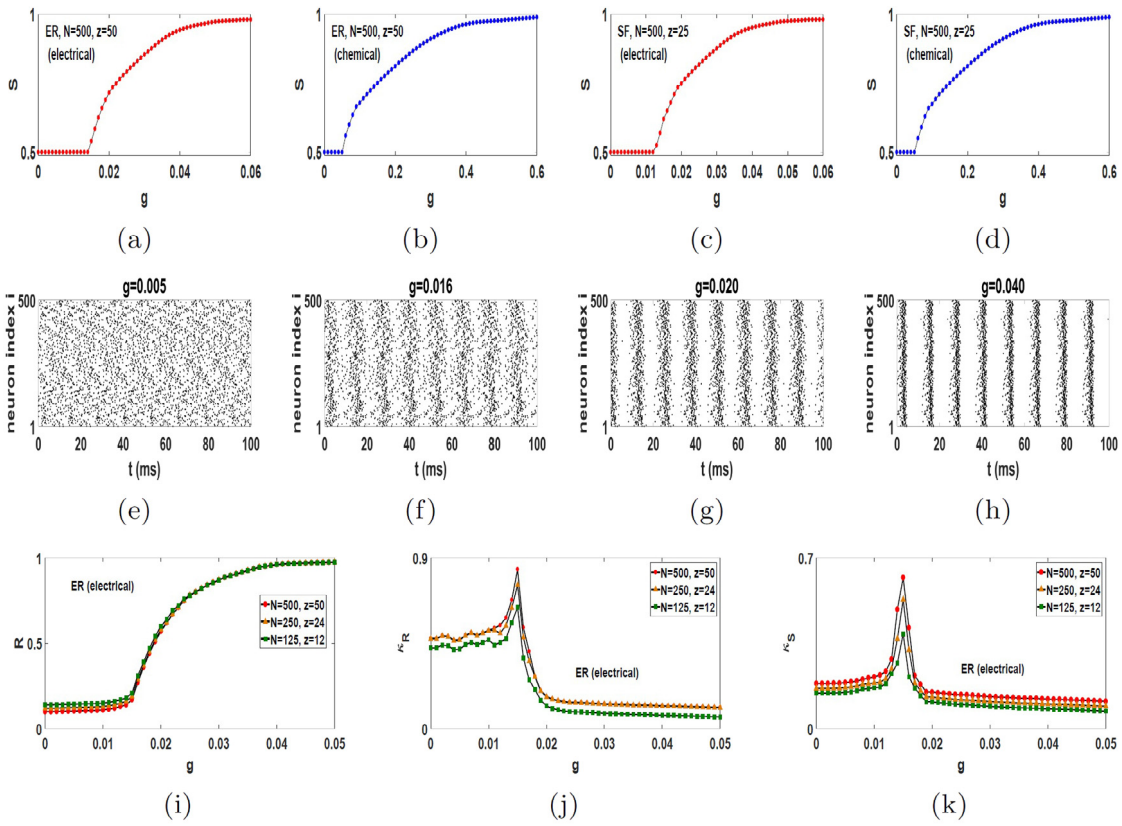


**Fig. 2.** (a) and (b) Transition to phase synchronization in ER networks of spiking HH neurons with electrical and chemical synapses. (c) and (d) Transition to phase synchronization in SF networks of spiking HH neurons with electrical and chemical synapses. (e)–(h) Raster plots for ER network with electrical synapses for various values of $g$. (i) Kuramoto order parameter $R$ vs $g$ for ER networks of HH neurons with electrical synapses for different system sizes $N$. (j) and (k) $\kappa_R$ and $\kappa_S$ vs $g$ for the same systems as in (i). $z = 0.1N$ in each case. $t = 0$ indicates the beginning of stationary state. The synchronization diagrams and susceptibility plots show the averaged results over five network realizations and initial conditions.

structure as well as SF network which has a heterogeneous random structure [25]. Such networks are constructed using a configurational model [25]. The networks size is $N = 500$. The mean connectivity is $z = 50$ for ER network and $z = 25$ for SF network. Also the degree distribution function of SF network is $P(k) \sim k^{-\gamma}$ with $\gamma = 2.2$. The results for synchronization transition of HH neurons with electrical and chemical synaptic currents, on ER and SF are shown in Figs. 2(a–d). It is observed that the system with both types of synapses exhibits a continuous transition from asynchrony to synchrony. Raster plots of spikes for the ER network with electrical synapses are illustrated in Figs. 2(e–h). It is evident that since clustering coefficient is significantly reduced due to randomness (as compared to regular networks), neuronal clusters do not appear in the system. However, presence of a significant number of long-range connections regulates neural activity in this random network when $g$ is increased above a certain threshold. Raster of spikes for other transitions are qualitatively similar to those of Figs. 2(e–h) (not shown). Looking at the value where the transition occurs, $g_t$, for a given network, one concludes that synchronization is more conducive to electrical synapses than chemical synapses, i.e. $g_t$ is about an order of magnitude smaller for electrical synapses. This makes sense as electrical synapses are known to be stronger than chemical synapses. On the other hand, the strong similarity between the results for ER and SF networks for a given synaptic type, including their corresponding value at transition, leads one to conclude that the role of structural heterogeneity (SF network) is not an important factor in influencing the type and shape of transition curves ($S - g$ plots).

In Fig. 2(i), we also show $R - g$ plots of HH neurons with electrical synapses on ER networks with three system sizes $N$ to be compared with the $S - g$ plot in Fig. 2(a). Here, $z = 0.1N$ in each system size. Furthermore, variations of the generalized susceptibilities $\kappa_R$ and $\kappa_S$ upon increasing $g$ for the systems of Fig. 2(i) are plotted in Figs. 2(j) and 2(k), respectively. It is observed that both $\kappa_R$ and $\kappa_S$ show a specific peak at the transition point which grows with increasing the system size. The behavior of the generalized susceptibilities further collaborates our order parameter results which indicate that our model does not show synchronization transition for low dimensional systems (Fig. 1), but exhibits definitive and continuous transition in a high dimensional structure such as complex networks (Fig. 2).

Regarding the results associated with Figs. 1 and 2, we can conclude two important points: (i) the main results are unaltered upon increasing the system size $N$, and (ii) the synchronization diagrams exhibit qualitatively the same behavior whether we employ $R$ or $S$, except for the more refined statistics provided by $S$ which enables us to determine the transition point clearly. Therefore, for the rest of this paper we report the results only based on the order parameter $S$ and for our largest available system size ($N \simeq 500$).

### 4.3. Small-world networks

After considering regular networks with high clustering but large average distance on one hand, and highly random networks with strong small-world effect but negligible clustering on the other hand, we are interested in networks that have high clustering coefficient, as well as small-world property. Therefore, we constructed Watts–Strogatz (WS) networks [25] with size $N = 500$ and the mean connectivity $z = 50$ by random rewiring

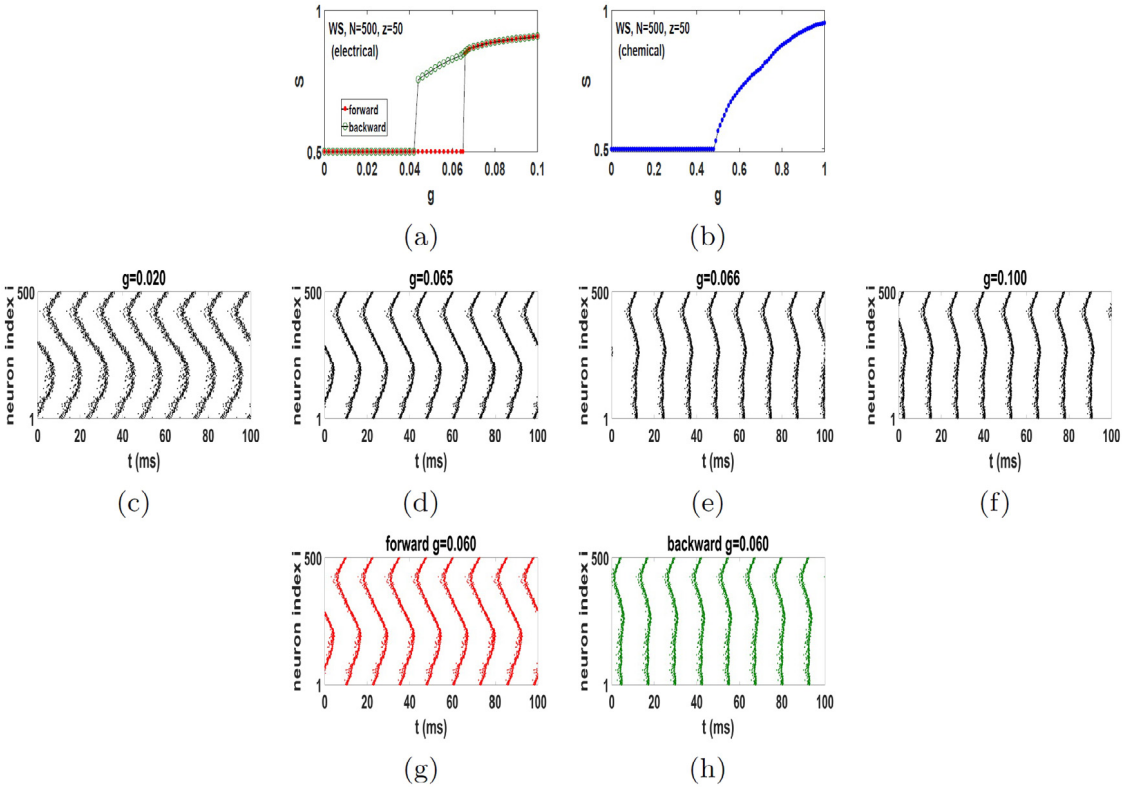


**Fig. 3.** Transition to phase synchronization in WS networks of spiking HH neurons with (a) electrical and (b) chemical synapses. Network size and coordination number are $N = 500$ and $z = 50$, respectively and rewiring probability is $p = 0.02$. (c)–(f) Raster plots for the network with electrical synapses for various values of $g$ of the system in forward direction. (g) and (h) Two raster plots for the same value of $g$ inside the hysteresis loop ($g = 0.060$) in forward and backward evolution of the system. $t = 0$ indicates the beginning of stationary state. The synchronization diagrams show the averaged results over five network realizations and initial conditions.

of two percent of links of a regular ring. This low rewiring probability ($p = 0.02$) allows the system to keep its large clustering coefficient while developing significantly low average distance (i.e. small-world effect). The resulting $S - g$ curves for WS networks with electrical and chemical synapses are shown in Figs. 3(a) and 3(b), respectively. Interestingly, we observe a discontinuous (explosive) transition for the case of electrical synapses while a continuous transition is observed for the chemical synapses. As we will discuss shortly, this type of explosive synchronization is different in its mechanism than those seen for phase oscillators in heterogeneous networks such as [56,57]. The synchronization transition is accompanied with a hysteresis loop if a backward sweep in $g$ is performed from the highly synchronized state. Therefore, as seen in Fig. 3(a), not only the transition is explosive, the value of $S$ is also history-dependent. This is to be contrasted with the case of chemical synapses in WS network where increasing $g$ leads to a continuous transition from asynchrony to synchrony in neural spiking as is clear in Fig. 3(b).

Therefore, one- and two-dimensional regular networks produced no transition, while random networks produced a continuous transition. However, small-world networks which lie somewhere between randomness and regularity exhibit explosive synchronization (electrical) as well as continuous transition (chemical). The fact that transition type in WS network depends on the interaction type is an interesting result and may be important from the point of view of neuroscience, since it has been reported that the brain networks at the microscopic level are similar to WS networks [58]. To elucidate the effect of topology and underlying reason for different order of phase transitions, we display the raster plots of HH neurons with electrical synapses on a WS network in Fig. 3(c–f) for the evolution of system in the forward direction. Here, the combined effect of clustering and long-range interaction leads to explosive synchronization. As in the regular rings case the effect of clustering leads initially to correlated regions which are nevertheless not perfectly synchronized for faraway regions of the network. Note the similarity in Figs. 1(g) and 3(d), both of which lead to $S = 0.5$ and no net synchronization. However, as the effect of long-range links in the case of WS network is important, increasing $g$ will eventually lead to interactions among various parts of the network which eventually leads to global order in the system and therefore a phase transition, which was absent in models without long-range interaction. But, why do we observe an explosive synchronization for electrical synapses but a continuous transition for chemical synapses? This has to do with the fact that long-range links provide strong interactions for the case of electrical synapses as phase difference of faraway regions is considerable, while providing weak interaction for local interactions which are mostly synchronized. When nonlocal regions suddenly go in synchronization due to strong electrical interactions a sudden jump in order parameter is observed. This is shown in Figs. 3(d) and 3(e) for the two consecutive values of $g$ ($g = 0.065$ and $g = 0.066$), at the edge of transition as global order suddenly arises in the system. On the other hand, in the case of chemical synapses, a pre-synaptic neuron interacts with a post-synaptic neuron in a decaying fashion thus providing a weaker effect which allows various regions of the network to slowly synchronize with each other and thus lead to a smooth continuous phase transition. Therefore, in the case of chemical synapses phase lags among various clusters vanish gradually (not shown). In Figs. 3(g) and 3(h), we plot raster plots within the hysteresis loop for the same value of $g$, one for the forward branch and one for the backward branch. Here, we note how small changes in global patterns of spikes can lead to significant change in the value of $S$.

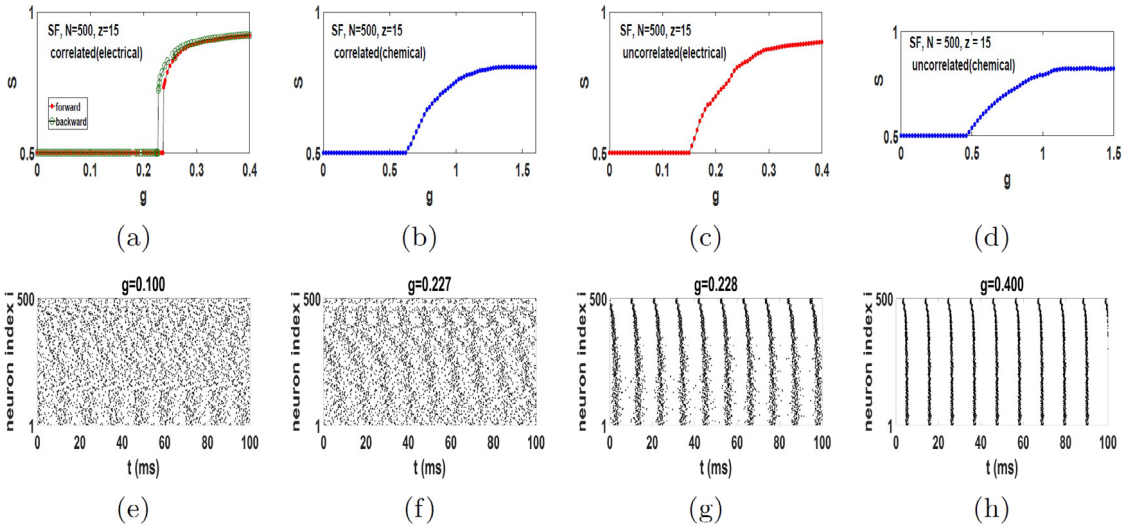


**Fig. 4.** Synchronization diagram for the correlated scale-free network (a) electrical synapses and (b) chemical synapses, and the corresponding uncorrelated case (c) and (d). Raster plots for various $g$ are shown in parts (e)–(h) for the case of explosive synchronization in panel (a). $t = 0$ indicates the beginning of stationary state. The synchronization diagrams show the averaged results over five network realizations and initial conditions.

### 4.4. Correlated heterogeneity

It might have been expected that heterogeneity in network structure as in the SF network in Fig. 2(b) would have led to a different transition pattern when compared to homogeneous random network of ER. We note that the importance of the role of heterogeneity in neural networks has attracted much attention in recent literature. An important observation in regard to synchronization in the Kuramoto model was that structural heterogeneity was not sufficient to lead to different transitional pattern, but a *correlation* between the frequency and the degree of the node was the key element that would lead to explosive synchronization in SF networks [56]. This means that the high frequency nodes in a network are also the highly connected nodes, while the low frequency nodes are sparsely connected. We note that the range of frequency in spiking HH neurons is relatively limited. However, one may attempt to make a heterogeneous distribution even in this limited range. We have therefore studied a SF network of size $N = 500$ with $\gamma = 2.2$ and $k_{min} = 7$, $k_{max} = 47$, and the mean connectivity $z = 15$. We have also produced the same distribution of frequencies with $f_{min} = 70$ Hz and $f_{max} = 110$ Hz and have studied the correlated ($f \propto k$) and the uncorrelated distribution of such frequencies. The results are shown in Fig. 4. As is seen, the correlated case leads to explosive synchronization along with hysteresis in the case of electrical synapses, but a smooth transition in the case of chemical synapses. We also show the same results for the uncorrelated case which indicates that the explosive synchronization is in fact due to the correlation between the two heterogeneous distributions of degree and frequency, in the case of electrical synapses.

It is interesting to note that the mechanism for explosive synchronization is very different here than that observed in WS network for electrical synapses. There, it was the combined effect of local order, which is achieved for low synaptic weight $g$, and long-range order which sets in for large values of synaptic weight, that leads to sudden order and explosive synchronization in the system, see raster plots in Fig. 3. Here, in the case of correlated heterogeneity, the system is still essentially in a completely disordered phase just before the explosive synchronization occurs. See $g = 0.227$ and $g = 0.228$ raster plots in Fig. 4 which are just before and after the explosive synchronization transition point. This indicates that the system truly goes through a sudden change from disordered to ordered phase. The cause of such an explosive synchronization can easily be understood by looking at the ordered raster plots. One sees that in the synchronous phase the entire system is oscillating at the frequency of $f \approx 110$ Hz which is exactly the frequency of the only hub in the system. This indicates the essential role of the hub in this explosive synchronization. The entire network must adjust with the hub and once this happens an explosive synchronization occurs. This mechanism is very much similar to what happens in the case of the well-known explosive synchronization in the Kuramoto model [56]. However, we emphasize that the explosive synchronization we have observed only occurs for the stronger electrical synapses, and we did not observe any explosive synchronization for chemical synapses in the range of parameters studied here. We finally note that explosive synchronization occurs at much higher values of $g$ when compared to the WS case and also exhibits a smaller hysteresis loop.

### 4.5. Hierarchical modular networks

So far we have investigated synchronization transition of spiking HH neurons for the most typical network topologies. However, it is believed that a hierarchical modular (HM) network is a more realistic representation of the actual structural connectivity of the cortex on the large scale [58]. Therefore it is worthwhile to investigate synchronization of HH neurons in HM networks as well. We construct networks with size $N = 512$, the mean connectivity $z = 15$ and 4 hierarchical levels, see Fig. 5(a). On the lowest level, the network is comprised of 16 modules of 32 nodes where each node is connected to 10 randomly chosen other nodes within the same module. On the second level, there are 8 modules which are constructed by connecting pairs of randomly chosen nodes belonging to two smaller modules of the lower level. In this manner we construct each module in a higher level by connecting members of two modules in the previous level. We should note that all links in the first level are inter-modular and all links in higher levels are intra-modular. This network despite having considerable clustering also has small-world effect.

$S - g$ plots for HH neurons with electrical and chemical synapses for such a HM network is displayed in Figs. 5(b) and 5(c), respectively. We observe that for both types of synapses, there exist three regimes in the $S - g$ plots. An asynchronous

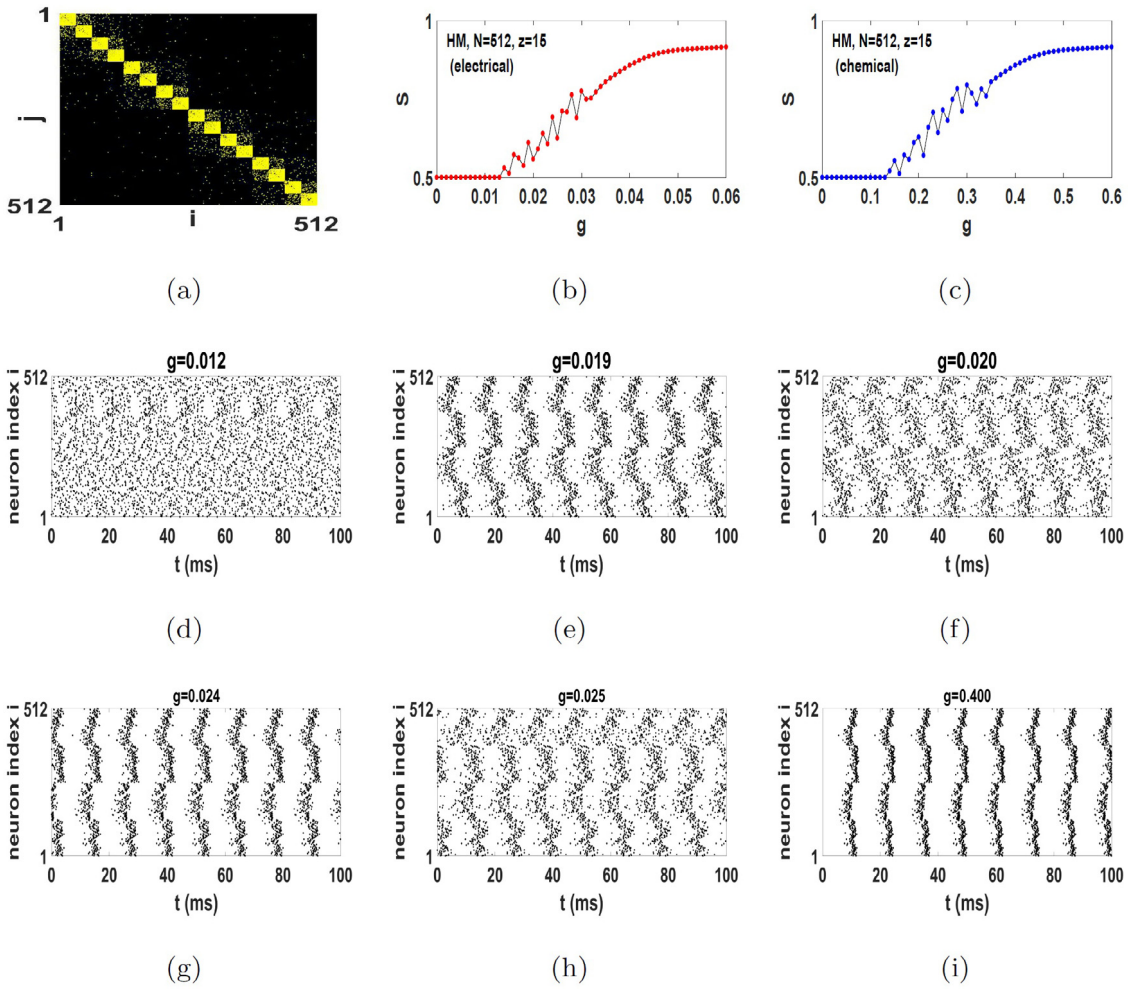


**Fig. 5.** (a) Adjacency matrix of the HM network of size $N = 512$, coordination number $z = 15$. There are 4 hierarchical levels. 16 modules in level 1, 8 modules in level 2, 4 modules in level 3 and 2 modules in level 4. (b) and (c) Synchronization diagram for electrical and chemical synapses, respectively. (d)–(i) Raster plots for neural network with electrical synapses for six different values of $g$. $t = 0$ indicates the beginning of stationary state. The synchronization diagrams show the averaged results over five network realizations and initial conditions.

regime ($S = 0.5$) for small values of $g$, a synchronous regime for large values of $g$ and an intermediate regime between ordered and disordered phases where $S$ does not vary monotonically with increasing $g$, but reveals a fluctuating behavior. Note that these fluctuations in order parameter are not due to insufficient transient time because we have made sure that the system is in its stationary state before taking measurement of $S$ for each value of $g$. They also do not appear due to imprecise numerical integrations as we have taken much care in this regard. Emergence of this intermediate regime has been reported for the Kuramoto model on human connectome network which has a hierarchical modular structure [59]. It is now believed that such intermediate regime is a manifestation of HM structure of the underlying network. As can be deduced from the raster plots in Figs. 5(d–i), the HM structure leads to synchronization within various modules which are themselves out of phase with various other modules leading to relative synchrony (small $S$) which nevertheless fluctuates as various modules go in and out of phase with each other as we change the value of $g$. For example, for electrical synapses and $g = 0.019$ there is more synchronization than $g = 0.020$ as can clearly be seen why from the corresponding raster plots. Therefore, we observe the same type of *frustrated* synchronization patterns as in the Kuramoto model regardless of the synaptic interaction. We also note that, looking at the values of transition point $g_t$, one sees strong similarity with fully random networks of SF and ER (see Fig. 2). This indicates that the onset of synchronization here is also dictated by long-range links. But, once synchronization sets in, it is the strong clustering within various modules that dictate the synchronization pattern for a range of $g$, before global order sets in for large enough $g$.

## 5. Concluding remarks

In a previous work, we studied beta-band synchronization in network models of spiking neurons. There, we showed that the type of synchronization transition occurring in a neural network depends on the firing rates of constituent neurons [24]. In this paper we have reported a systematic study of synchronization transition in network models of spiking neurons in gamma-band. We employed HH neurons with electrical and chemical synapses. Our focus has been to characterize the combined effect of synaptic type and topological features on the type of synchronization transitions that may occur. The mechanisms and patterns of synchronization transitions we obtained here for gamma-rhythms are distinctly different from those we obtained for beta-rhythms in Ref. [24]. For example, in the beta-band in a one-dimensional lattice, we found a continuous transition for the electrical synapses, while here for the gamma-band we observed no transition for any synaptic type in one or two dimensions. Furthermore, here we

found smooth transitions for SF and ER networks in the gamma-band, while previously we had observed explosive synchronization on such networks with electrical synapses. On the other hand, here we observe explosive synchronization for the WS networks while in the beta-band we only saw a smooth transition for such networks. We also observed explosive synchronization in the case of SF networks with correlated heterogeneity which was not studied in the previous study for the beta-band.

The underlying mechanisms leading to explosive synchronization in beta-band was rooted in the formation of anti-phase groups of neurons for intermediate values of $g$ and their sudden combination at a transition point [24]. This is distinctly different from the mechanism that lead to explosive synchronization in WS network of HH neurons or from the mechanism resulted in abrupt transition in SF network of HH neurons with correlated heterogeneity. However, these three mechanisms of explosive synchronization have a common aspect. They all occur through electrical synapses. We have not observed explosive synchronization in the case of chemical synapses. Our results highlight the fact that electrical synapses are more conducive to synchronization and can in fact lead to entirely different transition patterns. On the other hand, there is evidence that chemical and electrical synapses have similar synchronization patterns [38]; therefore, in the light of our results, further investigation of similarities and differences of such synaptic interactions seem to be in order.

We also note that it is interesting that our regular one and two dimensional lattice did not exhibit a transition which is what one would expect from the study of the Kuramoto model as it, too, does not exhibit a transition in low dimensional systems [48]. However, the mechanism for such behavior are different, as we do observe considerable amount of order in our system with quasiperiodic oscillations. We once again emphasize the key role of frequency as well as synaptic interactions in such studies, where in the beta-band, in one dimension, we had previously observed a continuous transition for the electrical synapses while no transition was seen for the chemical synapses.

This brings us to emphasize the difference in the type of transitions we observed in WS networks. Electrical synapses, which are strong and fast, lead to explosive synchronization while the slower and weaker chemical synapses lead to a smooth transition. This is particularly interesting as neuronal networks are argued to be on the verge of a phase transition. This could, for example, be related to the fact that electrical synapses are useful in fast involuntary motor response where a strong and fast collective action is desired, while a smooth transition with chemical synapses could be understood in terms of cortical neurons where too much synchronization is deemed to be pathological [22].

Furthermore, we investigated the role of correlated heterogeneity and found that in the case of electrical synapses one observes explosive synchronization while in chemical synapses a smooth transition occurs. This result could be interesting from two aspects. First, it shows that unlike what is generally believed, correlated heterogeneity does not always lead to explosive synchronization as chemical synapses showed a smooth transition. Secondly, it highlights the distinctly different type of explosive synchronization that may occur in electrical synapses. In WS network, explosive synchronization occurred *after* the system gained a high degree of local order, but in the case of correlated heterogeneity, explosive synchronization was dictated by the role of the hub with no sign of order in the system just before the transition occurred.

We have also considered hierarchical modular networks which resulted in an intermediate regime between order and disorder. Such a behavior has been previously shown to occur in the Kuramoto model [59] and our results indicate that such frustrated transition is a more general property of neuronal systems in HM networks, and it is furthermore independent of the type of synaptic interaction.

We note that our choice of spiking HH neurons naturally limited our range of frequency to the gamma band. However, we observed the same type of synchronization patterns when we increased the natural spiking frequency of the HH neurons to the high gamma band up to $f \approx 110$, not shown here. We previously observed that the synchronization patterns changed in the case of Izhikevich neurons when one increased the average frequency from beta to gamma band [24]. This was shown to be due to the dependence of refractory period on the frequency of the neurons. There seems to be two important time scales in such problems. One is the firing time scale, which remains relatively constant with changing frequency, and the other is the refractory period which may change considerably with frequency. The ratio of these two time scales may have important consequences for the patterns of synchronization as has been argued in [24]. While for low frequency band of beta, this ratio changes considerably, in the high frequency band studied here, the ratio remains relatively constant.

The role of refractory period, conduction/axonal delays, as well as synaptic plasticity on synchronization patterns are all potentially interesting avenues for future studies [60]. Evidence for robust collective oscillations at criticality, where scale-invariant activity emerges in neural networks, is reported in recent experimental and theoretical studies [23,16,15]. Investigation of such coexistence at the edge of continuous and explosive transitions obtained in the current study is interesting, as well, although such investigation will be computationally expensive. One might also consider the role of external oscillatory input in such studies which has been recently shown to introduce critical oscillations in certain models of excitable nodes [61]. Lastly, the role of noise was absent in our studies. Noisy dynamics may add some important features to the collective dynamics including important effects in the nature of the phase transition [62].

## CRediT authorship contribution statement

**Mahsa Khoshkhou:** Data curation, Formal analysis, Software, Visualization, Writing. **Afshin Montakhab:** Conceptualization, Funding acquisition, Methodology, Supervision, Writing.

## Acknowledgments

Support from Shiraz University research council is kindly acknowledged. This work has been supported in part by a grant from the Cognitive Sciences and Technologies Council.

## References

[1] H.B. Callen, Thermodynamics and an Introduction to Thermostatistics, Wiley, New York, 1998.
[2] S.K. Ma, Modern Theory of Critical Phenomena, Routledge, 2018.
[3] G. Weisbuch, Complex Systems Dynamics, CRC Press, New York, 2018.
[4] A. Steyn-Ross, M. Steyn-Ross, Modeling Phase Transitions in the Brain, Springer, 2010.
[5] D. Markovic, C. Gros, Phys. Rep. 536 (2014) 41–74.
[6] P. Bak, C. Tang, K. Wiesenfeld, Phys. Rev. Lett. 59 (1987) 381.
[7] P. Bak, K. Chen, M. Creutz, Nature 342 (1989) 780–782.
[8] M.A. Munoz, Rev. Modern Phys. 90 (2018) 031001.
[9] D.R. Chialvo, Nature Phys. 6 (10) (2010) 744.
[10] P. Moretti, M.A. Munoz, Nature Commun. 4 (2013) 2521.
[11] S.A. Moosavi, A. Montakhab, A. Valizadeh, Sci. Rep. 7 (2017) 7107.
[12] M. Rohden, A. Sorge, M. Timme, D. Witthaut, Phys. Rev. Lett. 109 (6) (2012) 064101.
[13] B. Blasius, A. Huppert, L. Stone, Nature 399 (1999) 6734, 354.
[14] L. Stone, R. Olinky, A. Huppert, Nature 446 (2007) 7135, 533.
[15] S. di Santo, P. Villegas, R. Burioni, M.A. Munoz, Proc. Natl. Acad. Sci. USA 115 (7) (2018) 1356–1365.
[16] M. Khoshkhou, A. Montakhab, Front. Syst. Neurosci. 13 (73) (2019).

[17] A.J. Fontenele, et al., Phys. Rev. Lett. 122 (2019) 208101.
[18] F. Varela, J.P. Lachaux, E. Rodriguez, J. Martinerie, Nature Rev. Neurosci. 2 (2001) 229–239.
[19] A. Buehlmann, G. Deco, PLoS Comput. Biol. 6 (2010) e1000934.
[20] P. Esir, A. Simonov, M. Tsodyks, Front. Comput. Neurosci. 11 (2017) 21.
[21] J. Fell, N. Axmacher, Nature Rev. Neurosci. 2 (2001) 105–118.
[22] E.R. Kandel, J.H. Schwartz, T.M. Jessell, Principles of Neural Science, McGraw-Hill, New York, 2000.
[23] D. Gireesh Elakkat, D. Plenz, Proc. Natl. Acad. Sci. USA 105 (2008) 7576.
[24] M. Khoshkhou, A. Montakhab, Front. Comput. Neurosci. 12 (2018) 59.
[25] C. Gros, Complex and Adaptive Dynamical Systems, fourth ed., Springer-Verlag, Berlin Heidelberg, 2015.
[26] G. Buzsaki, Rhythems of the Brain, Oxford University Press, New York, 2006.
[27] X. Jia, A. Kohn, PLoS Biol. 9 (4) (2011) e1001045.
[28] J.A. Henrie, R. Shapley, J. Neurophysiol. 94 (2005) 479–490.
[29] P. Fries, D. Nikolic, W. Signer, Trends Neurosci. 30 (7) (2007) 309–316.
[30] J.R. Vidal, M. Chaumon, J. Kevin, O. Regan, C. Tallon-Baudy, J. Cogn. Neurosci. 18 (11) (2006) 1850–1862.
[31] P. Berens, G.A. Keliris, A.S. Ecker, N.K. Logothetis, A.S. Tolias, J. Cogn. Neurosci. 2 (2008) 199–207.
[32] J. Liu, W.T. Newsome, J. Neurosci. 26 (2006) 7779–7790.
[33] P. Fries, J.H. Reynolds, A.E. Rorie, R. Desimone, Science 291 (2001) 1560–1563.
[34] F. Roux, P.J. Uhihaas, Trends Cog. Sci. 18 (1) (2014) 16–23.
[35] E.P. Bauer, R. Paz, D. Pare, J. Neurosci. 27 (2007) 9369–9379.
[36] P.J. Uhlhaas, W. Singer, Neuron 52 (2006) 155–168.
[37] A.L. Hodgkin, A.F. Huxley, J. Physiol. 117 (1952) 500.
[38] T. Perez, G.C. Garcia, V.M. Eguiluz, R. Vicente, G. Pipa, C. Mirasso, PLoS One 6 (5) (2011) e19900.
[39] Y. Wang, D.T.W. Chik, Z.D. Wang, Phys. Rev. E 61 (2000) 740.
[40] O. Kwon, H.T. Moon, Phys. Lett. A 298 (2002) 319–324.
[41] O. Kwon, K. Kim, S. Park, H.T. Moon, Phys. Rev. E 84 (2011) 021911.
[42] Q. Wang, M. Perc, Z. Duan, G. Chen, Phys. Lett. A 372 (2008) 5681–5687.
[43] C. Park, R.M. Worth, L. Rubchinsky, Phys. Rev. E 83 (2011) 042901.
[44] C. Zhou, J. Kurths, Chaos 13 (1) (2003) 401–409.
[45] T. de L. Prado, S.R. Lopes, C.A.S. Batista, J. Kurths, R.L. Viana, Phys. Rev. E 98 (2014) 032818.
[46] C.A.S. Batista, R.L. Viana, F.A.S. Ferrari, S.R. Lopes, A.M. Batista, J.C.P. Coninck, Phys. Rev. E 87 (2013) 042713.
[47] Y. Kuramoto, Lecture Notes in Phys. 39 (1975) 420–422.
[48] J.A. Acebron, L.L. Bonilla, C.J. Perez Vicente, F. Retort, R. Spigler, Rev. Modern Phys. 77 (2005) 1.
[49] S.A. Moosavi, A. Montakhab, Phys. Rev. E 92 (2015) 052804.
[50] S.G. Lee, A. Neiman, S. Kim, Phys. Rev. E 57 (1998) 3292.
[51] A. A. Roth, M. van Rossum, Computational Modeling Methods for Neuroscientists, MIT Press, Cambridge, MA, 2009.
[52] A. Pikovsky, M. Rosenblum, G. Osipov, Physica D 104 (1997) 219.
[53] C. van Vreeswijk, Phys. Rev. E 54 (1996) 5522.
[54] M. Rosenblum, A. Pikovsky, Phys. Rev. Lett. 98 (2007) 064101.
[55] R. Burioni, S. Santo, M. Volo, A. Vezzani, Phys. Rev. E 90 (2014) 042918.
[56] J. Gomez-Gardenes, S. Gomez, A. Arenas, Y. Moreno, Phys. Rev. Lett. 106 (2011) 128701.
[57] I. Leyva, R. Sevilla-Escoboza, J.M. Buldu, I. Sendima-Nadal, J. Gomez-Gardenes, A. Arenas, Y. Moreno, S. Gomez, R. Jaimes-Reategui, S. Boccaletti, Phys. Rev. Lett. 108 (2012) 168702.
[58] O. Sporns, Networks of the Brain, The MIT Press, Cambridge, 2011.
[59] P. Villegas, P. Moretti, M.A. Munoz, Sci. Rep. 4 (2014) 5990.
[60] M.M. Asl, A. Valizadeh, P.A. Tass, Chaos 28 (2018) 106308.
[61] S.A. Moosavi, A. Montakhab, A. Valizadeh, Phys. Rev. E 98 (2) (2018) 022304.
[62] S.A. Moosavi, A. Montakhab, Phys. Rev. E 89 (2014) 052139.